Chemical Science

ROYAL SOCIETY OF CHEMISTRY

EDGE ARTICLE

View Article Online
View Journal | View Issue

Cite this: *Chem. Sci.*, 2020, **11**, 5526

All publication charges for this article have been paid for by the Royal Society of Chemistry

Received 12th December 2019
Accepted 12th May 2020

DOI: 10.1039/c9sc06300e

rsc.li/chemical-science

Examining the role of phosphorylation of p19^{INK4d} in its stability and ubiquitination using chemical protein synthesis†

Muna Msallam,‡ Hao Sun,‡ Roman Meledin, Pauline Franz and Ashraf Brik *

p19^{INK4d} plays an important role in the regulation of the cell cycle by inhibiting the function of cyclin-dependent kinases 4/6 that is responsible for the phosphorylation and deactivation of the retinoblastoma protein (pRb) tumour suppressor. Recently, it was reported that phosphorylation of p19^{INK4d} at Ser76 and Ser66 causes structural changes, which lead to its ubiquitination and degradation. Yet the exact contribution of each phosphorylation site remains unclear. To shed light on the role of these sites, we developed the chemical synthesis of unmodified, mono- and doubly phosphorylated p19^{INK4d} using state of the art methods for chemical protein synthesis. The synthesized proteins were characterized by circular dichroism and biochemical methods to examine the effect of phosphorylation on the thermal stability and ubiquitination, respectively. Our results provide clear determination of p19^{INK4d} stability upon phosphorylation at different sites and reveal that phosphorylation of both Ser residues might be necessary for promoting ubiquitination of p19^{INK4d}.

Introduction

p19^{INK4d} is a member of the INK4 family that includes p16^{INK4a}, p15^{INK4b} and p18^{INK4c} proteins.[1] The INK4 family shares a high degree of sequence and structural homology, which contributes to its function in regulating the cell cycle.[2] Specifically, this family induces cell cycle arrest through the inhibition of cyclin-dependent kinases 4/6 (CDK4/6) and prevents the formation of the CDK4/6-Cyclin D complex that deactivates the pRb tumour suppressor *via* its phosphorylation.[3,4] p19^{INK4d} is a 166 amino acid protein made of five ankyrin repeats of helices and beta-turns,[5,6] of which Ser66 and Ser76 residues undergo phosphorylation, while Lys62 was found to be ubiquitinated. Interestingly, among the INK4 family members, only p19^{INK4d} showed a high level of phosphorylation and exhibited rapid proteasome mediated-degradation *in vivo*.[7,8]

Balbach and coworkers proposed a crosstalk between p19^{INK4d} phosphorylation at Ser66 and Ser76 and its ubiquitination at Lys62.[9,10] The group prepared different analogues of p19^{INK4d} using a glutamic acid mimic of phosphoserine at Ser66 and Ser76 (S66E/S76E) and found that unlike S66E, S76E strongly destabilizes the protein; however for efficient ubiquitination both S66E and S76E are required.[9] More recently, the group enzymatically prepared p19^{INK4d} mono-phosphorylated at Ser66 and doubly phosphorylated at both Ser residues and studied the effect of phosphorylation on the p19^{INK4d} structure and ubiquitination.[10] Based on this study, the group proposed a mechanism where the stepwise phosphorylation, first at Ser66 using p38 kinase and then at Ser76 using CDK1 kinase, causes significant structural changes, leading to the dissociation of CDK4/6 and subsequent ubiquitination and degradation of p19^{INK4d}. However, phosphorylation of Ser76 could not be introduced separately and was only detected after Ser66 phosphorylation. Therefore, the exact effect of mono-phosphorylation of either Ser66 or Ser76 on both the thermal stability and ubiquitination of p19^{INK4d} is still not clear.

Chemical protein synthesis is a powerful approach to prepare homogeneous and workable amounts of proteins bearing post-translational modifications such as phosphorylation and ubiquitination, essentially, without restrictions on the number and sites of these modifications.[11,12] In addition, incorporation of modified amino acids during the chemical synthesis bypasses the need for the involvement of enzymes such as kinases, which in many cases are unknown for the specific protein. Therefore, we reasoned that by using protein chemical synthesis one could prepare phosphorylated p19^{INK4d} analogues, in particular phosphorylated p19^{INK4d} at Ser76, with high homogeneity and in workable quantities to shed light on its exact role.

Here we report the chemical synthesis of four different analogues of p19^{INK4d} including the non-phosphorylated **p19^{INK4d}(WT)**, the mono-phosphorylated at Ser66 or Ser76 **p19^{INK4d}(S^{P}66)**/**p19^{INK4d}(S^{P}76)** and the doubly phosphorylated **p19^{INK4d}(S^{P}66 & S^{P}76)**. The synthetic proteins were folded *in*

Schulich Faculty of Chemistry, Technion-Israel Institute of Technology, Technion City, Haifa 32000, Israel. E-mail: abrik@technion.ac.il

† Electronic supplementary information (ESI) available. See DOI: 10.1039/c9sc06300e

‡ These authors contributed equally.

vitro and characterized for their stabilities and ubiquitination levels. Our results clearly show that the stability of p19^{INK4d} is affected by the position of phosphorylation; moreover, phosphorylation of both of Ser residues might be required for higher stimulation of ubiquitination of p19^{INK4d}.

Results & discussion

Chemical synthesis of p19^{INK4d} analogues

Our strategy for the synthesis of p19^{INK4d} is outlined in Fig. 1, in which we divided the polypeptide sequence into three fragments (Fig. 1A); Cys-p19^{INK4d}(109-166) (fragment **1**), Thz-**p19^{INK4d}(S^{P}66 & S^{P}76)**(56-107)-thioester (fragment **2**), and p19^{INK4d}(2-54)-thioester (fragment **4**). All the fragments were prepared according to the Fmoc-SPPS strategy on a Rink-amide resin with the appropriate linker depending on the desired C-terminus functionality for each fragment. Fragment **2** was prepared using the 3-amino-4-(methylamino)benzoic acid linker (MeDbz) since it has a C-terminal Gly residue to afford the peptide with the *N*-acyl-*N*′-methylbenzimidazolinone (MeNbz) functionality, while fragment **4** which bears a C-terminal Thr residue was prepared using a Dbz linker to obtain the peptide with *N*-acylbenzimidazolinone (Nbz).[13,14] The thioester forms of these fragments were obtained by substituting the MeNbz and Nbz units with methyl 3-mercaptoproprionate (MMP), to allow a longer storage time and reduce hydrolysis during ligation. The N-terminal Ala residue in fragments **1** and **2** was replaced with Cys and thiazolidine (Thz), respectively, to allow native chemical ligation (NCL).[15,16]

Once these fragments were prepared in high yield and excellent purity, we performed NCL between fragments **1** and **2** under typical NCL conditions of 4-mercaptophenylacetic acid (MPAA) and tris(2-carboxyethyl)phosphine hydrochloride (TCEP) in 6 M Gn·HCl at pH 7. The ligation step was fast and completed within 1 h at 37 °C. The reaction mixture was then treated with $MgCl_2$ followed by $[Pd(allyl)Cl]_2$ for Thz-opening in a one-pot manner.[17] The reaction was completed within an hour (Fig. 1B), quenched with DTT and the crude mixture was purified by reversed-phase HPLC to obtain the ligated product in a 42% isolated yield (Fig. 1C). To obtain the full-length polypeptide, NCL between ligated peptide **3** and fragment **4** was executed, which required 24 h for completion because of the sterically hindered ligation site. Subsequently, the Cys residues were desulfurized by applying radical desulfurization conditions (TCEP, VA-044, and *t*BuSH) (Fig. 1D).[18] The desulfurized product was purified and lyophilized to obtain the synthetic **p19^{INK4d}(S^{P}66 & S^{P}76)** in ~18% yield. Using this chemical strategy, we synthesized all the p19^{INK4d} analogues in milligram quantities and excellent purity (Fig. 1E).

Folding of p19^{INK4d} analogues

While attempting the *in vitro* folding of p19^{INK4d} analogues, we encountered difficulties despite using different folding

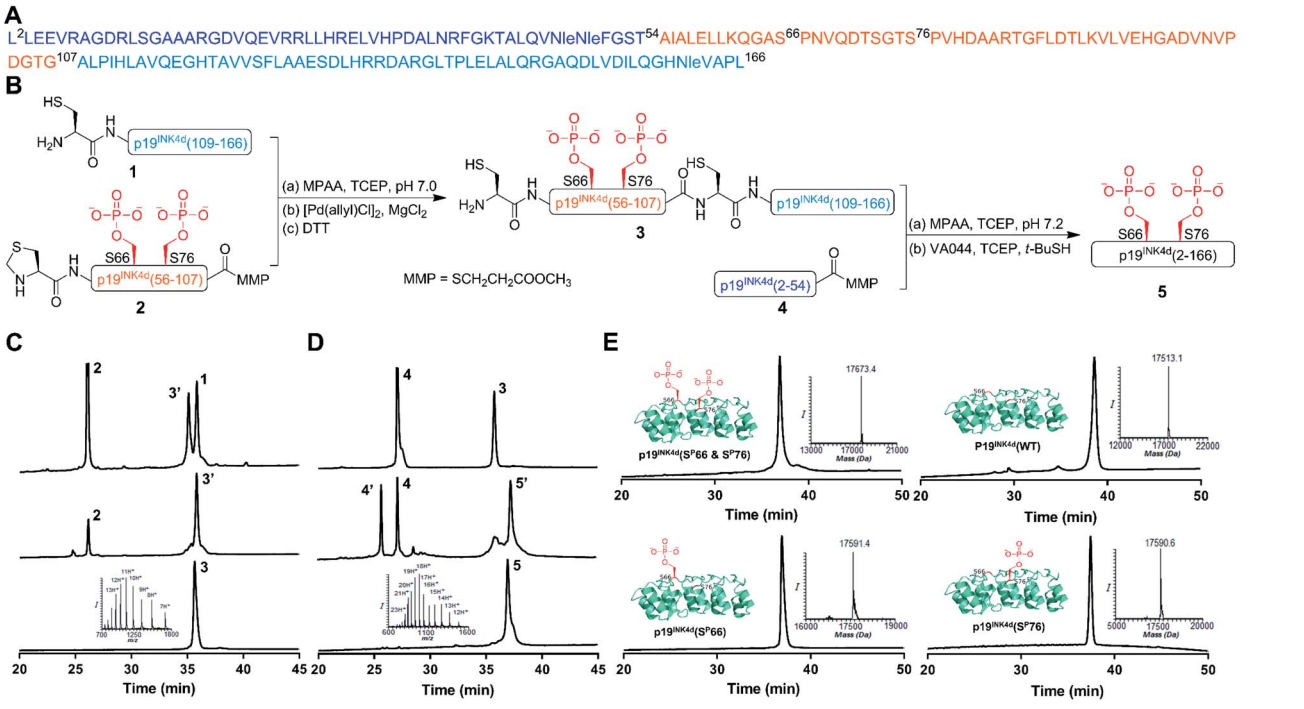

Fig. 1 General scheme for the synthesis of p19^{INK4d} analogues. (A) Sequence of p19^{INK4d}. Met49, Met50 and Met162 were replaced with Nle to avoid oxidation during the synthesis. (B) Synthetic strategy for obtaining **p19^{INK4d}(S^{P}66 & S^{P}76)**. (C) HPLC and mass analysis of ligation and Thz-opening to acquire **3**. (D) HPLC and mass results for final ligation and desulfurization steps to afford **5**, **p19^{INK4d}(S^{P}66 & S^{P}76)**. (E) HPLC and mass analysis of the purified analogues of p19^{INK4d}: **p19^{INK4d}(S^{P}66 & S^{P}76)** with an observed mass of 17 673.4 ± 2.1 Da (calculated 17 671.9 Da), **p19^{INK4d}(WT)** with an observed mass of 17 513.1 ± 2.1 Da (calculated 17 513.9 Da), **p19^{INK4d}(S^{P}66)** with an observed mass of 17 591.4 ± 2.1 Da (calculated 17 592.9 Da), and **p19^{INK4d}(S^{P}76)** with an observed mass of 17 590.6 ± 2.1 Da (calculated 17 592.9 Da).

conditions since we often observed precipitation of the protein over time both while diluting and during the circular dichroism (CD) measurements. Eventually, we found that dissolving the analogues in 6 M Gn·HCl followed by adding 50 mM sodium phosphate in 25% glycerol (pH 7.4 and final 2% Gn·HCl), which has been shown to increase the folding yield and reduce aggregation in various systems,[19,20] led to obtaining a clear solution of the protein ready for further characterization.

Secondary structure characterization and thermal stability analysis of p19^{INK4d} analogues

After successfully folding all the different synthetic analogues we attempted to determine the effect of phosphorylation on p19^{INK4d} thermal stability by monitoring the changes in the CD of each analogue upon increasing the temperature of the protein solution. Specifically, we followed the changes in the ellipticity at 208 nm and 222 nm – the signature of the alpha-helical secondary structure, upon increasing the temperature.[21,22]

At 10 °C, we observed the expected characteristic peaks for all the p19^{INK4d} analogues. Increasing the temperature to 25 °C did not induce any major changes in the CD signal. However, after a further increase in the temperature to 37 °C, we observed a significant decrease in the molar ellipticity curve for **p19^{INK4d}(S^{P}76)** and **p19^{INK4d}(S^{P}66 & S^{P}76)** (Fig. 2). We quantified this change for each analogue by calculating the alpha-helical content at both 25 °C and 37 °C using the Greenfield and Fasman equation.[23] The changes in the alpha-helical content from 25 °C to 37 °C for **p19^{INK4d}(WT)** and **p19^{INK4d}(S^{P}66)** analogues were 2.8% and 3.7% respectively. These changes were negligible compared to those of **p19^{INK4d}(S^{P}76)** and **p19^{INK4d}(S^{P}66 & S^{P}76)** analogues, which were 11.6% and 13.4% accordingly, thus indicating that the latter analogues are less stable than the former.

To further verify the thermal stability of the different analogues, thermal-denaturation scans were collected with a wider range of temperatures at both 222 nm and 208 nm. From the initial observation of the thermal-denaturation curves, we noticed similar thermal stability for **p19^{INK4d}(WT)** and **p19^{INK4d}(S^{P}66)** analogues and correspondingly for **p19^{INK4d}(S^{P}76)** and **p19^{INK4d}(S^{P}66 & S^{P}76)** (Fig. 3A). The melting temperature (T_m) of each analogue was determined, giving us direct evidence and accurate determination of their stabilities. The CD signal at 222 nm was converted to the folded fraction and the T_m at which the folded fraction was 0.5 was extrapolated using the Boltzmann fit (Fig. 3B).[21,24] The T_m values reported in Fig. 3C support our alpha-helical content change results and clearly indicate that **p19^{INK4d}(WT)** and **p19^{INK4d}(S^{P}66)** are much more stable analogues than **p19^{INK4d}(S^{P}76)** and **p19^{INK4d}(S^{P}66 & S^{P}76)** with more than 10 °C differences. Complementary results were obtained when calculating the T_m according to the CD signal at 208 nm wavelength (ESI, Fig. S20†). Our findings do not only suggest that there is a remarkable effect of phosphorylation on the p19^{INK4d} stability, but also uncover that phosphorylation of different Ser residues has a different effect on thermal stability, where phosphorylation at Ser76 significantly decreases p19^{INK4d} stability compared with Ser66 phosphorylation.

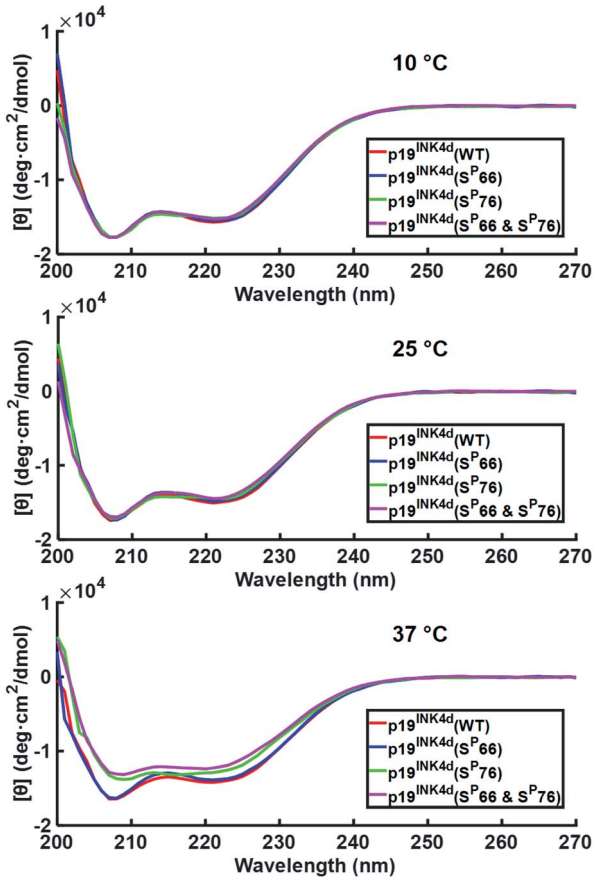

Fig. 2 CD analysis of p19^{INK4d} synthetic analogues where the CD signal is monitored at different temperatures; 10 °C, 25 °C, and 37 °C. Concentrations determined for this experiment were 7 μM for p19^{INK4d}(WT) and p19^{INK4d}(S^{P}66 & S^{P}76), and 5 μM for p19^{INK4d}(S^{P}66) and p19^{INK4d}(S^{P}76).

Additional H-D exchange experiments were performed for the four analogues to check any tertiary structural differences at room temperature, wherein the CD spectra of these analogues did not exhibit any secondary structure differences (ESI, Fig. S22†). The results show a higher rate of exchange for **p19^{INK4d}(S^{P}76)** and **p19^{INK4d}(S^{P}66 & S^{P}76)** analogues compared to **p19^{INK4d}(WT)** and **p19^{INK4d}(S^{P}66)**, reflecting tertiary structural changes even at room temperature. Since Ser76 phosphorylation seems to have an effect on the tertiary structure, these results agree with the CD analysis as well as support the previously reported 1H–15N 2D HSQC NMR study which has shown major structural changes upon the incorporation of the second phosphorylation at Ser76.[10]

Studying the crosstalk between phosphorylation and ubiquitination

Next, we wanted to study the crosstalk between phosphorylation and ubiquitination of our synthetic analogues. This would allow us to find out first, whether the ubiquitination level will change upon mono- or di-phosphorylation of p19^{INK4d} and second, if there are different effects of the phosphorylation positions on ubiquitination and correlate these results with the protein

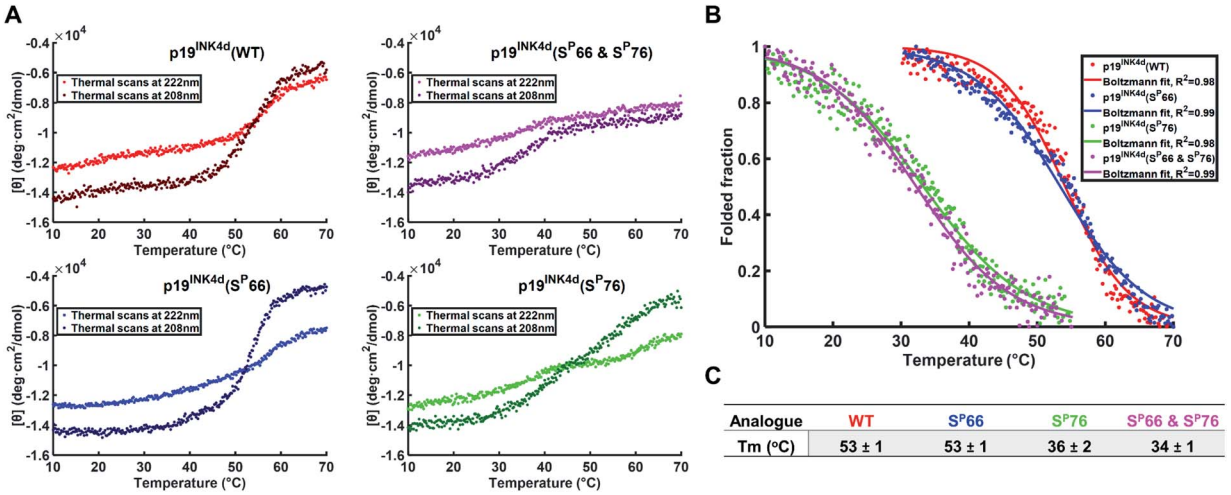

Fig. 3 Stability analysis of p19^{INK4d} analogues using CD. (A) Single measurement of thermal scans from 10 °C to 70 °C obtained for all the analogues of p19^{INK4d} at 222 nm and 208 nm wavelength. (B) Folded fraction plotted against temperature calculated using the Boltzmann equation to fit the sigmoidal curves obtained from thermal scans at 222 nm in Fig. 3A. (C) Mean T_m values ± SD °C of the four analogues acquired from three independent measurements for each analogue (ESI, Fig. S21†).

stability. To enable additional verification of the ubiquitination level, HA-tagged analogues were prepared. The synthesis of these analogues was performed according to the synthesis of the previous analogues; however, fragment **4** was prepared with an HA tag (ESI, Scheme S7, S16–S19†).

Since the E3 ligase of p19^{INK4d} has yet to be discovered, we used S-phase synchronized HeLa or U2OS cells as a source for the E3 enzyme. The analogues were loaded separately in four *in vitro* ubiquitination reactions, reacted simultaneously, and incubated at 37 °C for 1 h. The analogues can be distinguished through western blot by a slight but clear shift in gel migration, according to the difference in the number of phosphorylated residues. The doubly phosphorylated **HA-p19^{INK4d}(S^{P}66 & S^{P}76)** band appears slightly higher than the bands of mono-phosphorylated **HA-p19^{INK4d}(S^{P}66)**/**HA-p19^{INK4d}(S^{P}76)** analogues while the latter migrate higher than the band of **HA-p19^{INK4d}(WT)**. Phosphorylation or dephosphorylation of the different analogues can thus be monitored throughout the ubiquitination assay and since the dephosphorylation of **HA-p19^{INK4d}(S^{P}66 & S^{P}76)** was observed, the phosphatase inhibitor was added to the lysis buffer to prevent it (Fig. S23†). The signal of HA-p19^{INK4d} polyubiquitin conjugate bands for HeLa cells is reasonably low after 1 h (Fig. S24†) but can be seen for a similar assay performed using S-phase U2OS cells, with the incorporation of p38 and CDK1 kinase inhibitors (Fig. 4). Based on Fig. 4 and S26,† in comparison to **HA-p19^{INK4d}(WT)**, **HA-p19^{INK4d}(S^{P}66 & S^{P}76)** and **HA-p19^{INK4d}(S^{P}66)** exhibited increased ubiquitination of 62 ± 22% and 14 ± 7% respectively, while **HA-p19^{INK4d}(S^{P}76)** ubiquitination was reduced by 8.9 ± 2%, indicating that phosphorylation at Ser76 is not enough for efficient ubiquitination.

Based on these results, we suggest that phosphorylation at both Ser66 and Ser76 might potentially promote the ubiquitination of p19^{INK4d}. We also suggest that other factors might be involved in the productive ubiquitination of p19^{INK4d}. Thullberg *et al.* suggested, for instance, that the association with CDK4, even in its mutant form, determines the efficient ubiquitination of p19^{INK4d}, by notably increasing the ubiquitination level.[8]

Phosphorylation among other effects can either inhibit or induce ubiquitination and stability is often referred to as a linking bridge towards understanding the effect of phosphorylation on ubiquitination.[25] Phosphorylation that stabilizes the protein can lead to a decrease in ubiquitination such as in the case of MDM2 phosphorylation *via* PKB, or otherwise, cause destabilization and increase ubiquitination as in the case of p53 phosphorylation by aurora kinase A.[26,27] In the case of p19^{INK4d}, based on the results presented here, phosphorylation at different positions have an eminently different effect on

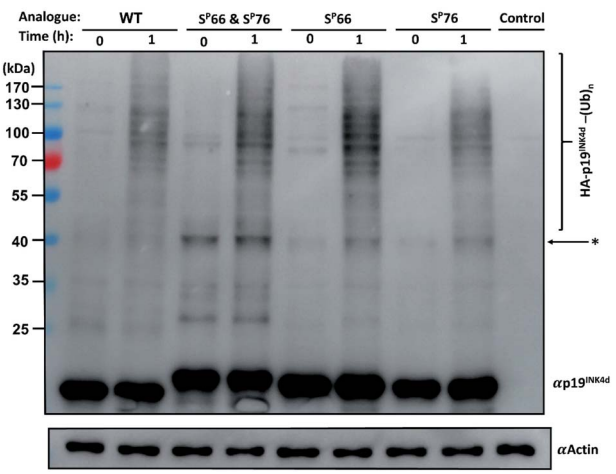

Fig. 4 Ubiquitination study of HA-p19^{INK4d} analogues. Immunoblot of each synthetic analogue of HA-p19^{INK4d} with addition of S-phase U2OS lysate obtained before incubation in 37 °C (0 h) and after 1 h. The control contained assay compounds with cell lysate. Actin is shown below as a loading control. *Unidentified bands which can correspond to impurity and poly-ubiquitinated p19^{INK4d}.

stability, where phosphorylation at Ser76, unlike phosphorylation at Ser66, causes major destabilization of $p19^{INK4d}$ but its sole incorporation is not enough for inducing efficient ubiquitination. Phosphorylation at both Ser66 and Ser76 might be required for the recognition of the E3 ligase, which triggers a higher ubiquitination signal of $p19^{INK4d}$.

Conclusions

In this work, we report the first total chemical synthesis of $p19^{INK4d}$ protein – **$p19^{INK4d}$(WT)** along with its phosphorylated analogues; **$p19^{INK4d}(S^P66$ & $S^P76)$**, **$p19^{INK4d}(S^P66)$** and the **$p19^{INK4d}(S^P76)$** analogue that was not obtained using enzymatic approaches. We were able to determine by measuring the T_m for the different synthetic analogues, the changes in the thermal stability of $p19^{INK4d}$ upon phosphorylation of Ser66 or/and Ser76 residues, where we show that **$p19^{INK4d}(S^P76)$** and **$p19^{INK4d}(S^P66$ & $S^P76)$** have similar low stability while **$p19^{INK4d}(S^P66)$** does not affect the stability as the calculated T_m is identical compared to **$p19^{INK4d}$(WT)**. While **$p19^{INK4d}(S^P76)$** causes major thermal destabilization, our *in vitro* ubiquitination study reveals that it is not sufficient for inducing a high polyubiquitination signal. However **$p19^{INK4d}(S^P66$ & $S^P76)$** induces the highest ubiquitination signal supporting the mechanism suggested by the Balbach group.[10,28] Since polyubiquitination was also detected for the other analogues, we suggest that other factors might affect ubiquitination and should be taken into consideration such as the direct interaction with CDK4/6. Also, since the phosphorylation of both Ser residues occurred at the Ser-Pro junction, S-phase lysate may contain enzymes such as peptidyl-prolyl *cis–trans* isomerases (PPIas) that assist the proper folding of $p19^{INK4d}$. Although the use of prolyl isomerase was mentioned before for folding $p19^{INK4d}$ to its native-like order structure *in vitro*, its function was not reported *in vivo*.[29,30] Apart from the possible involvement of these enzymes in folding $p19^{INK4d}$, there are various enzymes essential for understanding the functional pathway of $p19^{INK4d}$ that have still not been identified, such as the ligase and the phosphatases. Finding the specific E3 ligase, for example, would aid in minimizing variables during *in vitro* ubiquitination assay performed with lysate. Our synthetic route for the different analogues opens the door for proteomic analysis to unravel these enzymes and other unknown aspects of $p19^{INK4d}$ biology.

Conflicts of interest

The authors declare no conflict of interest.

Acknowledgements

This project has received funding from the European Research Council (ERC) under the European Union's Horizon 2020 research and innovation programme (grant agreement no. [831783]). A. B. holds The Jordan and Irene Tark Academic Chair. We thank Dr Sumeet K. Singh for his contribution in peptide synthesis.

Notes and references

1 F. K. Chan, J. Zhang, L. Cheng, D. N. Shapiro and A. Winoto, *Mol. Cell. Biol.*, 1995, **15**, 2682–2688.
2 R. Baumgartner, C. Fernandez-Catalan, A. Winoto, R. Huber, R. A. Engh and T. A. Holak, *Structure*, 1998, **6**, 1279–1290.
3 E. T. Cánepa, M. E. Scassa, J. M. Ceruti, M. C. Marazita, A. L. Carcagno, P. F. Sirkin and M. F. Ogara, *IUBMB Life*, 2007, **59**, 419–426.
4 M. F. Roussel, *Oncogene*, 1999, **18**, 5311–5317.
5 F. Y. Luh, S. J. Archer, P. J. Domaille, B. O. Smith, D. Owen, D. H. Brotherton, A. R. C. Raine, X. Xu, L. Brizuela, S. L. Brenner and E. D. Laue, *Nature*, 1997, **389**, 999–1003.
6 W. Kalus, R. Baumgartner, C. Renner, A. Noegel, F. K. M. Chan, A. Winoto and T. A. Holak, *FEBS Lett.*, 1997, **401**, 127–132.
7 M. Thullberg, J. Bartkova, S. Khan, K. Hansen, L. Rönnstrand, J. Lukas, M. Strauss and J. Bartek, *FEBS Lett.*, 2000, **470**, 161–166.
8 M. Thullberg, J. Bartek and J. Lukas, *Oncogene*, 2000, **19**, 2870–2876.
9 C. Löw, N. Homeyer, U. Weininger, H. Sticht and J. Balbach, *ACS Chem. Biol.*, 2009, **4**, 53–63.
10 A. Kumar, M. Gopalswamy, A. Wolf, D. J. Brockwell, M. Hatzfeld and J. Balbach, *Proc. Natl. Acad. Sci. U. S. A.*, 2018, **115**, 3344–3349.
11 S. Bondalapati, M. Jbara and A. Brik, *Nat. Chem.*, 2016, **8**, 407–418.
12 S. S. Kulkarni, J. Sayers, B. Premdjee and R. J. Payne, *Nat. Rev. Chem.*, 2018, **2**, 0122.
13 J. B. Blanco-Canosa and P. E. Dawson, *Angew. Chem., Int. Ed.*, 2008, **47**, 6851–6855.
14 J. B. Blanco-Canosa, B. Nardone, F. Albericio and P. E. Dawson, *J. Am. Chem. Soc.*, 2015, **137**, 7197–7209.
15 P. E. Dawson, T. W. Muir and S. B. H. Kent, *Science*, 1994, **266**, 776–779.
16 V. Agouridas, O. El Mahdi, V. Diemer, M. Cargoët, J. C. M. Monbaliu and O. Melnyk, *Chem. Rev.*, 2019, 119.
17 M. Jbara, S. K. Maity, M. Seenaiah and A. Brik, *J. Am. Chem. Soc.*, 2016, **138**, 5069–5075.
18 Q. Wan and S. J. Danishefsky, *Angew. Chem., Int. Ed.*, 2007, **46**, 9248–9252.
19 R. V Rariy and A. M. Klibanov, *Proc. Natl. Acad. Sci. U. S. A.*, 1997, **94**, 13520–13523.
20 F. Corrêa and C. S. Farah, *Biophys. J.*, 2007, **92**, 2463–2475.
21 N. J. Greenfield, *Nat. Protoc.*, 2007, **1**, 2527–2535.
22 N. J. Greenfield, *Nat. Protoc.*, 2007, **1**, 2876–2890.
23 N. Greenfield and G. D. Fasman, *Biochemistry*, 1969, **8**, 4108–4116.
24 A. M. Brown, *Comput. Methods Progr. Biomed.*, 2001, **65**, 191–200.
25 T. Hunter, *Mol. Cell*, 2007, **28**, 730–738.
26 J. Feng, R. Tamaskovic, Z. Yang, D. P. Brazil, A. Merlo, D. Hess and B. A. Hemmings, *J. Biol. Chem.*, 2004, **279**, 35510–35517.

27 H. Katayama, K. Sasai, H. Kawai, Z. M. Yuan, J. Bondaruk, F. Suzuki, S. Fujii, R. B. Arlinghaus, B. A. Czerniak and S. Sen, *Nat. Genet.*, 2004, **36**, 55–62.
28 Phosphorylation using CDK1 kinase occurred in the **p19^{INK4d}(S^{P}66)** analogue only, confirming the stepwise phosphorylation mechanism suggested by the Balbach group, see Fig. S28,† page 51.
29 M. Zeeb, H. Rösner, W. Zeslawski, D. Canet, T. A. Holak and J. Balbach, *J. Mol. Biol.*, 2002, **315**, 447–457.
30 C. Löw, U. Weininger, M. Zeeb, W. Zhang, E. D. Laue, F. X. Schmid and J. Balbach, *J. Mol. Biol.*, 2007, **373**, 219–231.